Nucleic Acids Research

OXFORD Journals online

 822-829

Hairpin-dimer equilibrium of a parallel-stranded DNA hairpin: formation of a four-stranded complex

Utz Dornberger , Joachim Behlke[2] , Eckhard Birch-Hirschfeld[1] and Hartmut Fritzsche*

Institut für Molekularbiologie and [1] Institut für Virologie, Friedrich-Schiller-Universität, Winzerlaer Straße 10, D-07745 Jena , Germany and [2] Max-Delbrück-Zentrum für Molekulare Medizin, Robert-Rössle Straße 10, D-13122 Berlin -Buch, Germany

Received October 15, 1996; Revised and Accepted January 6, 1996

ABSTRACT

The 24mer deoxyoligonucleotide 3 ' -d$(T)_{10}$- 5' -5' -d$(C)_4$ - d$(A)_{10}$- 3' (psC4) with an uncommon 5' -p-5' phosphodiester linkage was designed to enable the formation of a hairpin structure with unusual parallel-stranded stem. As reference hairpin structure with an antiparallel-stranded stem, the 24mer 5' -d$(T)_{10}$ -d$(C)_4$ -d$(A)_{10}$ -3' (apsC4) was chosen. The behaviour of these oligonucleotides at different temperatures, DNA and salt concentrations was characterised by a combination of UV melting, CD, CD melting, infrared and Raman spectroscopy, infrared melting and analytical ultracentrifugation. The parallel-stranded hairpin structure was found to be formed by psC4 only under conditions of low DNA concentration and low salt concentration. Increase of the NaCl concentration beyond the physiological level or high DNA concentration supports the formation of intermolecular multi-stranded structures. The experimental data are in agreement with a four-stranded complex formed by two molecules of psC4. The base pairing model of this asymmetric four-stranded complex is based on the pyrimidine motif of a triple helix with two bifurcated hydrogen bonds at the O4 of the thymine each directed towards one of the amino protons of both adenines. In contrast, the reference oligonucleotide apsC4 forms only an antiparallel-stranded hairpin under all experimental conditions.

INTRODUCTION

The antiparallel orientation of complementary strands in right-handed A- and B-form and left-handed Z-form helices is a fundamental structural principle of DNA structure that shapes its physical and biological capacity. However, 10 years ago, it was predicted that d$(A)_6$ [middot]d$(T)_6$ might form a parallel-stranded, right-handed double helical structure with reverse Watson-Crick base pairing (1). Recently several authors have published their experimental results (2 - 9) which demonstrate the existence of a parallel double-stranded

helix (ps DNA) in solution. The sequence constraints for the formation of ps DNA in these systems were obtained, either by using oligonucleotides containing tracts of A and T residues (2 , 3) or by the introduction of alternating AT or GA segments (4 , 5). Beside parallel-stranded duplexes, a special 24mer DNA oligonucleotide 3'-d$(T)_{10}$ -5'-5'-d$(C)_4$ -d$(A)_{10}$ -3' (psC4) with an uncommon 5'-p-5' phosphodiester linkage in the loop between the T and C residues was designed to facilitate the formation of an intramolecular hairpin structure (Fig. 1 A) with a parallel-stranded stem (ps hairpin) (6 , 8). Low DNA concentration and temperature >20°C were found to favour the parallel-stranded hairpin (ps hairpin) formation. Considering investigations of ps hairpin formation by the very similar DNA oligonucleotide 3'-d$(T)_8$ -5'-5'-d$(C)_4$ -d$(A)_8$ -3', the formation of multimeric antiparallel-stranded structures was proposed at DNA concentration higher than 2.5 mM (8 , 9).

Figure 1 . (**A**) Intramolecular parallel-stranded hairpin (ps hairpin). Possible intermolecular structures of psC4: (**B**) parallel-stranded duplex; (**C**) antiparallel-stranded structure (potential for forming concatamers); (**D**) triplex structure; (**E**) four-stranded complex and (**F**) multimeric chain of four-stranded complexes. (**G**) Intramolecular antiparallel-stranded hairpin (aps hairpin). (I) Watson-Crick; ([circle]) *reverse* Watson-Crick; (*) Hoogsteen base pairing.

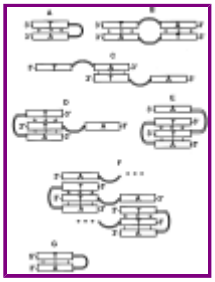

It has been shown that DNA sequences with fully and partly matched palindromic sequences can exist in solution in equilibrium between two ordered forms identified as the monomeric hairpin and the dimeric duplex structure (10 - 15). The hairpin-dimer equilibrium is shifted to the intramolecular hairpin conformation at low DNA concentration and high temperatures, whereas the increase of the ionic strength favors the formation of the intermolecular dimer. While several structural and thermodynamic aspects of hairpin-dimer equilibrium have been investigated for hairpins with the stem in the B or Z conformation (14 , 15), the behaviour of hairpin structures with parallel-stranded stems has not been thoroughly studied.

We used UV absorption spectroscopy, circular dichroism (CD), analytical ultracentrifugation, Fourier transform infrared (FT-IR) and Raman spectroscopy to describe the equilibrium between the ps hairpin and the intermolecular structure of the oligonucleotide psC4 considering different ionic strengths, DNA concentrations and temperatures. The results are compared to an antiparallel-stranded hairpin, 5'-d$(T)_{10}$ -d$(C)_4$ -d$(A)_{10}$ -3' (apsC4), which is devoid of the 5'-p-5' phosphodiester linkage and has the stem in B conformation (Fig. 1 G).

MATERIALS AND METHODS

Materials

Oligodeoxynucleotides psC4 and apsC4 were synthesized by using automated phosphoramidite chemistry on a DNA synthesizer (Applied Biosystems Model 394). 5'- *O* -dimethoxytrityl-2'-deoxynucleoside-3'- *O* -(2-cyanoethyl- *N* , *N* -diisopropyl) aminophosphanes were purchased from Perseptive Biosystems GmbH and 5'-CE-phosphoramidite from GLEN Research. The standard solutions for activation, oxidation and detritylation were also from these companies. Supports consisted of a thin layer (3-5%) of polystyrene grafted onto a polytetrafluoroethylene core (16). Polymer-supported

oligonucleotides were cleaved from supports and deprotected by treatment with 28% aqueous ammonia solution for 6-12 h at 55^{o}C. Purification was carried out on a BioRad Model 2700 system using a mono Q HR5/5 anion-exchange column from Pharmacia. The salt content was adjusted to ~1 Li per phosphate by $LiClO_4$ precipitation and elution on a Sephadex G10 column. The sample purity was checked by 15% polyacrylamide gel electrophoresis under denaturing conditions (8 M urea, 90 mM Tris-borate, 5 mM EDTA, pH 8.3, stained by 0.4 [mu]g/ml ethidium bromide and visualized by fluorescence). Experiments were carried out with samples dissolved in 10 mM Na-cacodylate, pH 7.2 (unless stated otherwise) to which various amounts of NaCl or $MgCl_2$ were added, as indicated. In all experiments, samples were heated at 75^{o}C for 5 min and slowly cooled to room temperature after each addition of salt. D_2O was purchased from Aldrich.

Optical spectroscopy

The UV absorption measurements were performed on a Cary 1E spectrophotometer (Varian) equipped with a thermostated cell holder. The molar extinction coefficients of the oligonucleotides at 260 nm and 80^{o}C were apsC4, 8900 M^{-1} cm^{-1} ; psC4, 9000 M^{-1} cm^{-1} and $pd(T)_{10}$, 8800 M^{-1} cm^{-1} (6). All concentrations are designated on a per oligomer basis unless otherwise mentioned.

The thermal denaturation was followed at four different wavelengths: 257, 260, 266 and 280 nm. The heating rate was 0.5^{o}C/min. Changes in the heating or cooling rates (0.2-1.0 ^{o}C/min) did not affect the thermodynamic parameters. Absorbance readings were collected at 0.25^{o}C intervals in the temperature range 8-85^{o}C.

CD spectra were recorded on a Jasco Model 720 CD dichrograph using 1 cm path length cell. The sample temperature was controlled by circulating water bath. Spectra reported are averages of two scans. The CD melting curves were collected at 0.5^{o}C intervals between 2 and 85^{o}C.

Thermal denaturation analysis

The data from the thermal transition experiment were analyzed according to a concerted two-state model for the helix to coil transition as described by Ramsing *et al* . (17). The initial parameters for T_m and $[Delta]H_{vH}$ at each wavelength were determined from a derivative plot of the thermal transition curve computed with Savitzky-Golay filters. The linear parameters $[epsilon]_0^h$, $[beta]^h$, $[epsilon]_0^c$ and $[beta]^c$ were estimated from for the two linear segments of the thermal transition curves (17). The initial parameters were improved by the non-linear least-squares minimization routine based on the Levenberg-Marquardt algorithm using Tablecurve 2D from Jandel Scientific.

Analytical ultracentrifugation

Molecular mass of the oligonucleotides was determined by sedimentation equilibrium experiments using an analytical ultracentrifuge XL-A from Beckman. About 70 [mu]l of the samples dissolved in 10 mM Na-cacodylate buffer, pH 7.2, containing different amounts of NaCl were filled in the chamber of six-channel cells and centrifuged 2 h at 36 000 r.p.m. (overspeed) followed by 20 h at 30 000 r.p.m. (equilibrium speed) at different temperatures between 5 and 40^{o}C. The radial concentration distribution at sedimentation equilibrium was

recorded with 10 repeats at three different wavelengths, mostly using 255, 260 and 265 nm. Molecular mass (M) of the oligonucleotides was obtained from the radial concentration distribution (c_r) by a non-linear fitting procedure according equation **1** using our program Polymol (18). $c_r = c_{ro}$ @exp[MK(r^2 - {roman r} sub {roman o} sup 2) **1** with {roman K} = {{(1 - {roman {rho {v bar}}}) {{roman omega} sup 2}} over {2 {roman {R T}}}} **2**

or from the linear fit d ln c/d(r^2) by equation **3** {roman M} = {{2 {roman {R T}}} over {(1 - {roman {rho {v bar}}}) {{roman omega} sup 2}}} cdot {{{roman d} ln {roman c}} over {{{{roman d} ({roman r}} sup 2})}} **3**

R is the gas constant, T the absolute temperature, [omega] the angular velocity and c_{ro} the concentration at the radial reference position. The data for the buoyancy term (1 - {roman {rho {v bar}}}) were taken as Equation values from Cohen and Eisenberg (19).

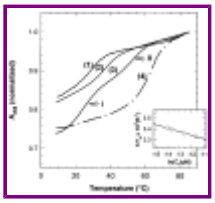

Figure 2 **.** UV melting curves. (**1**) psC4 in 20 mM NaCl. (**2**) psC4 in 100 mM NaCl. (**3**) psC4 in 1 M NaCl. (**4**) apsC4 in 1 M NaCl. All experiments were done in 10 mM Na-cacodylate, pH 7.2. Oligomer concentration: 1.2-2.0 [mu]M. Insert: dependence of the melting temperature of transition I on psC4 concentration in 1 M NaCl, 10 mM Na-cacodylate, pH 7.2.

FT-IR spectroscopy

FT-IR measurements were performed using a Bruker IFS-66 FT-IR spectrometer equipped with MCT and DGTS detectors. The DNA solutions were placed in a demountable temperature-controlled liquid cell (Harrick) with CaF_2 windows. Path lengths were 6 [mu]m for samples in H_2 O buffer and 6 or 56 [mu]m for samples in D_2 O buffer. The resolution was set to 2 cm^{-1} , 32 interferograms were accumulated and coadded, and Fourier-transformed using the Happ/Genzel apodization function. The DNA spectrum was obtained by subtraction of the buffer spectrum from the spectrum of the DNA solution at the respective temperature. The unsmoothed DNA spectra were used for further analysis. Standard procedure of Fourier deconvolution of the spectra was carried out (20) and performed by using Lorentzian bandwidth of 13 cm^{-1} and a resolution enhancement factor 2. Thermal studies were carried out at a linear heating rate of 0.75^{o}C/min while recording 32 interferograms in 1 min. Plots of intensity at 1625 cm^{-1} versus temperature and band position of the C=O stretching vibration around 1695 cm^{-1} versus temperature were evaluated from the original spectra at 0.75^{o}C temperature intervals. These plots show the thermal transition of the helix to the coil state. The transition temperature was determined using the first derivative of the transition curves. The DNA triple helix was prepared by direct mixing of the oligonucleotide apsC4 with decadeoxythymidylate, pd(T)$_{10}$, in aqueous solution. About 1.5 [mu]l droplets of these samples were deposited in cells equipped with ZnSe windows.

Raman spectroscopy

Glass capillary tubes with the DNA oligomer solutions were mounted directly in the sample illuminator of the Raman spectrometer (Jobin Yvon T 64000) equipped with a CCD detector. Raman spectra were excited with the 488 nm line of an argon laser (Innova 90,

Coherent Inc.) using 100 mW of radiant power at the sample.

RESULTS

UV melting experiments

The melting curves and hyperchromicity profiles of the oligonucleotide psC4 (Fig. 2, curves 1 and 2, and Fig. 3) in buffer with NaCl concentration of <= 100 mM determined by UV absorption spectroscopy were characteristic of ps DNA, in according to previous studies (6, 17). UV melting analysis of psC4 in the presence of 100 mM NaCl reveals a cooperative monophasic melting transition with T_m = 38.8°C and [Delta]H_{vH} = 190 kJ/mol. The corresponding values for the reference hairpin apsC4 are T_m = 49.5°C and [Delta]H_{vH} = 209 kJ/mol. Figure 3 A shows the hyperchromicity profile of psC4 and apsC4 at the same NaCl concentration (100 mM). The relative absorption increase due to helix-coil transition displays a strong wavelength dependence that is in the case of psC4 characteristic for ps DNA (6, 17).

Figure 3 . Hyperchromicity profiles. Absorbances of the oligonucleotide at 85°C were divided by the absorbance of the same samples at 9°C. (**A**) apsC4 (dashed line) and psC4 (solid line) in 100 mM NaCl. (**B**) apsC4 (dashed line) and psC4 (solid line) in 1 M NaCl. All experiments were done in 10 mM Na-cacodylate, pH 7.2. Oligomer concentration: 1.2-2.0 [mu]M.

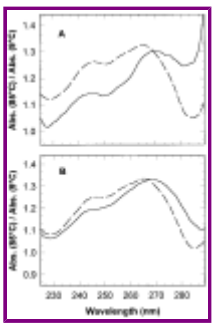

A clear biphasic melting curve was observed for psC4 upon increase of the NaCl concentration above 100 mM. Curve 3 of Figure 2 shows the melting curve of psC4 in the presence of 1 M NaCl. The midpoint (T_m) of the higher temperature transition (transition II) is independent of the oligomer concentration, while the midpoint of the lower temperature transition (transition I) does show a dependence (see insert of Fig. 2). On cooling both transitions are fully reversible. The hyperchromicity profile of psC4 at 1 M NaCl approaches the features characteristic for antiparallel-stranded DNA (6, 8, 17) (Fig. 3 B). The same behaviour of psC4 was observed in buffers with $MgCl_2$ concentrations above 2 mM. The reference oligonucleotide apsC4 shows a monophasic melting curve at all ionic strength with thermal transition independent from the oligomer concentrations. This picture is consistent with (i) an intramolecular ps hairpin-coil equilibrium for transition II of psC4; (ii) an intermolecular structure-ps hairpin equilibrium for transition I of psC4 and (iii) aps hairpin-coil equilibrium for apsC4.

CD spectroscopy

PsC4 exhibits slight differences in the CD spectral range 230-290 nm in comparison with the reference hairpin apsC4 in a buffer with 100 mM NaCl. In particular the CD difference spectra (psC4-apsC4) show positive peaks at 247 nm and negative peaks at 260 and 284 nm (Fig. 4 A) in accordance with previous studies (6, 8). Smaller difference peaks were observed upon increase of the NaCl concentration between 230 and 290 nm (Fig. 4 A), while a stronger negative peak at 217 nm occurs. Duplex structures are characterized by a positive peak whereas triplexes exhibit mainly a negative peak between 200 and 230 nm

(21). Thus, the strong decrease of the intensity of the peak at 217 nm could reflect the formation of triple helical structure by psC4 at higher NaCl concentrations. Therefore, we measured the CD melting curves at 217 nm to follow the melting of the supposed triple helix. Figure 4 B shows the CD melting curve of psC4 at 217 nm in a buffer with 1 M NaCl. The CD-derived T_m (21.4^{o}C) for the observed transition between 2 and 40^{o}C is identical with the T_m (22.4^{o}C) of transition I in the UV melting curve. Between 40 and 90^{o}C the [Delta][epsilon] value of the CD melting curves decreases both for psC4 and apsC4. The results suggest formation of an intermolecular triple helix by two psC4 molecules as the intermolecular structure of psC4 at high NaCl concentration.

Figure 4 . CD spectra and CD melting curves. (**A**) CD difference spectra (psC4-apsC4) at different NaCl concentrations: 100 mM (dashed line), 400 mM (dotted line) and 1 M (solid line). (**B**) CD melting curve at 217 nm, ([circle]) apsC4 and (-) psC4 in 1 M NaCl. All experiments were done in 10 mM Na-cacodylate, pH 7.2 at 8^{o}C. Oligomer concentration: 3.0 [mu]M.

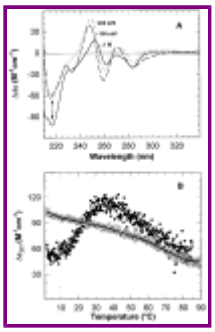

Analytical ultracentrifugation

Sedimentation equilibrium runs were carried out at different NaCl concentrations for psC4 as well as apsC4. The radial concentration distribution for psC4 in 100 mM NaCl at 5^{o}C is presented as linear slope d ln c/d(r^2) in Figure 5 A. From these values a molecular mass of 8350 Da was calculated using equation **3**. This result exceeds the monomeric molecular mass of 7860 somewhat indicating a weak association. In comparison to psC4 the slope obtained for apsC4 is something lower resulting in a molecular mass of 7800 Da. When increasing the salt concentration we get higher molecular masses for psC4 as derived from Figure 6 . In the presence of 1 M NaCl values of 15 400 " 200 were obtained, suggesting nearly all psC4 molecules are involved in intermolecular dimer formation. In contrast to this behaviour apsC4 remains in the monomeric state even at the high salt concentration (Fig. 5 B).

Figure 5 . Sedimentation equilibrium ultracentrifugation. Radial concentration distribution of psC4 ([circle]) and apsC4 ([Delta]) given as d ln c/d(r^2) at sedimentation equilibrium at (**A**) 100 mM NaCl and (**B**) 1 M NaCl. Experiments were done in 10 mM Na-cacodylate, pH 7.2 at 5^{o}C. Oligomer concentration: 1.0 [mu]M.

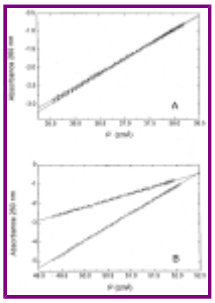

Figure 6 . Influence of NaCl and temperature on the molecular mass of 1.0 [mu]M solution psC4. The curves from top to bottom belong to the following NaCl concentrations: 1 M, 830 mM, 660 mM, 600 mM, 400 mM, 300 mM, 180 mM and 100 mM.

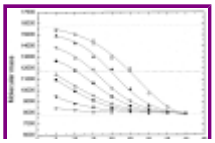

At a low temperature of 5^{o}C we can observe the strong influence of the NaCl concentration on the monomer-dimer transition of psC4. With increasing temperature the differences decline and disappear at nearly 40^{o}C where only monomers are observed (Fig. 6). This dissociation reaction is fully reversible (data not shown). This observation shows clearly a salt- and temperature-dependent transition between a ps hairpin and an intermolecular dimeric structure of psC4.

FT-IR spectroscopy

Striking differences between the spectra of psC4 and apsC4 were found in the region of the C=O stretching vibration at 1650-1700 cm^{-1} at 1 mM oligomer concentration. The infrared spectra of the D_2 O solutions of psC4 and apsC4 show a frequency shift of the vibration bands at 1663 cm^{-1} and 1697 cm^{-1} of the antiparallel-stranded reference hairpin apsC4 to new band positions of the psC4 at 1665, 1688 and 1696 cm^{-1} , respectively (Fig. 7 , curves 1 and 2). These values of psC4 are in very good agreement with the band position of the C=O stretching vibrations of the parallel-stranded duplex ps-D1D2 (Fig. 7 , curve 3) indicating the formation of a ps hairpin by psC4 at 1 mM oligomer concentration (22). No further differences in the infrared spectra of the ps hairpin and the aps hairpin were found in D_2 O or H_2 O solution (data not shown).

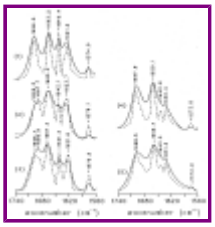

Figure 7 **.** Infrared spectra in D_2 O between 1740 and 1560 cm^{-1} . (**1**) apsC4 and (**2**) psC4 in D_2 O, pD 7.6 at 5^{o}C (1 mM oligomer). (**3**) ps-D1D2 in 150 mM NaCl, 30 mM $MgCl_2$, pD 7.6 at 20^{o}C (see ref. 22). (**4**) psC4 and (**5**) apsC4 plus single strand $d(T)_{10}$ (triple helix) in D_2 O, 1 M NaCl, pD 7.6 at 25^{o}C (12 mM oligomer). The Fourier deconvoluted spectra are shown as dotted lines. Band positions correspond to deconvoluted spectra.

Upon increase of the DNA concentration above 1.5 mM oligomer and/or addition of NaCl we observed significant changes in the infrared spectra of psC4. Curve 4 of Figure 7 shows the infrared spectra of psC4 at 12 mM oligomer and 1 M NaCl in the region between 1740 and 1560 cm^{-1} compared with the spectra of the triple helix apsC4*$p(dT)_{10}$ under the same conditions (curve 5). The position of the vibration bands of psC4 and the triple helix apsC4*$p(dT)_{10}$ are nearly identical in this frequency region. The hairpin apsC4 can form a triple helix with $p(dT)_{10}$ attaching the single strand to the double helical stem $d(A)_{10}$ -$d(T)_{10}$ by hydrogen bonds of the Hoogsteen type (pyrimidine motif) (23). Formation of this kind of DNA triple helix is indicated in the infrared spectra by a shift of the C=O stretching vibration at 1663-1659 cm^{-1} , an appearance of a new thymine band at 1630 cm^{-1} (24 , 25), and an almost complete disappearance of the adenine band at 1622 cm^{-1} (Fig. 7). The same vibrational bands were observed in the infrared spectra of psC4 at high oligomer concentration (Fig. 7 , curve 4). The two bands at 1643 and 1630 cm^{-1} could be assigned to the ring vibration of the thymine involved in Watson-Crick and Hoogsteen base pairing, respectively (25). In the Fourier deconvoluted infrared spectra of psC4, these two bands have a similar integrated intensity suggesting that roughly 50% of the thymines are involved in Watson-Crick and the other 50% in Hoogsteen base pairing. Interestingly we observed only a very small intensity of the band around 1622 cm^{-1} in the infrared spectra of psC4 as

well as in the infrared spectra of the triple helix apsC4*p(dT)$_{10}$. This band could be assigned to the combined vibration of the ring and the ND$_2$ group of adenine and cytosine.

In summary, the features of the infrared spectra of psC4 at oligomer concentration of >1 mM and/or high NaCl concentration mentioned above may account for a formation of an intermolecular multi-stranded structure based on a triple helix by psC4.

Figure 8 shows plots of the intensity at 1625 cm^{-1} and the band position of C=O stretching vibration versus temperature. These bands reflect the hairpin-coil transition of apsC4 and the intermolecular multi-stranded structure-coil transition of psC4. For both oligonucleotides we observed a monophasic transition. The thermodynamic analysis (17) of the temperature-dependent intensity at 1625 cm^{-1} of apsC4 reveals a T_m value of 64.6^{o}C and a [Delta]H$_{vH}$ value of 204 kJ/mol. This is in good agreement with thermodynamic parameters (T_m = 63.9^{o}C, [Delta]H$_{vH}$ = 206 kJ/mol) of the hairpin-coil transition determined by UV melting curves. The monophasic character of the IR melting curves of psC4 and apsC4 indicates that both oligonucleotides form predominantly uniform structures also at such high oligomer concentrations.

Figure 8 . IR melting curves of apsC4 ([circle]) and psC4 (-) in 1 M NaCl, oligomer concentration: 12 mM. (**A**) Plot of the adenine vibration located around 1625 cm^{-1} as a function of temperature. (**B**) Plot of band position of thymine C=O stretching vibration as a function of temperature.

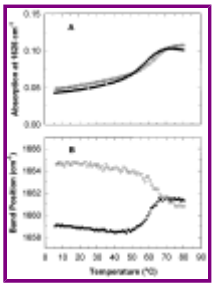

Raman spectroscopy

The Raman spectrum of psC4 in H$_2$ O displays a less intensive band at 1346 cm^{-1} relative to the band at 1377 cm^{-1} as compared with the spectra of apsC4 (data not shown). The band at 1346 cm^{-1} is mainly due to the NC8H/NC2H bending mode of adenine (26). For triple helices of poly(U*A-U) type, interaction at the N7 position was identified by a decrease in the intensity of the 1344 cm^{-1} band (26). This finding supports the intermolecular multi-stranded helix formation by psC4 like derived from the infrared spectra.

DISCUSSION

The data reported in this paper give a new insight to the hairpin- dimer/multimer equilibrium of parallel-stranded hairpins. In previous studies, it was already suggested that parallel-stranded hairpins can form higher order antiparallel-stranded structures at increased salt or oligonucleotide concentration (4 , 7 - 9). Especially for the DNA oligonucleotide p3'-d(T)$_8$ - 5'-5'-d(C)$_4$ -d(A)$_8$ -3', the formation of concatameric structures in the conventional antiparallel manner (Fig. 1 C) was proposed at DNA concentration higher than 2.5 mM (8 , 9). Our experimental results are more consistent with a transition from parallel-stranded hairpin to dimeric multi- stranded structures by psC4 upon increase of ionic strength or DNA concentration.

Hairpin-dimer equilibrium

The biphasic melting profile of psC4 at high salt concentrations, combined with the results of the sedimentation experiments, offer strong experimental evidence that this oligonucleotide can adopt both the parallel-stranded hairpin and intermolecular dimer structure. According to the melting experiments in buffers with 1 M NaCl, the oligonucleotide psC4 exists at room and lower temperatures in an equilibrium between intermolecular structure and ps hairpin since the melting profile of this molecule is biphasic and the transition I is concentration dependent. Several alternative intermolecular structures of the oligonucleotide (Fig. 1 B-F) are compatible with these results. Therefore, we investigated the intermolecular structure-ps hairpin equilibrium of psC4 by sedimentation experiments to obtain more definite information about the intermolecular structure. Ross *et al* . reported the utility of the sedimentation equilibrium experiments to study the duplex-hairpin equilibrium of conventional antiparallel-stranded hairpins (27). Our study is based on the assumption that the partial specific volumes and the number of bound cations do not differ for the intermolecular and hairpin structure of psC4. Even when this assumption is not strictly fulfilled our data clearly show that the molecular weight of the intermolecular structure is equivalent to two molecules of psC4, representing a dimeric structure.

The CD melting experiments gave us more information about the strand orientation of the dimeric structure of psC4. Several authors used the increase of CD signal at 217 nm to detect the triplex to duplex transition in CD melting curves (21 , 28 , 29). Perfectly formed triple helix structures like dT*dA-dT show a negative peak at 217 nm. The dimeric structure formed by psC4 at high salt (1 M NaCl) and low temperature (8^{o}C) shows a positive CD signal at 217 nm, but the disruption of the dimeric structure is accompanied by a strong increase of the CD amplitude at 217 nm in the CD melting curve (Fig. 4 B). Moreover the CD signal at 217 nm goes to higher values as one traverses the temperature range in which the first UV melting event occurs. Thus, we concluded that the dimeric structure of psC4 could probably represent a multi-stranded structure based on a triple helix according to the pyrimidine motif (Fig. 1 D or E).

It has been shown that most of the synthetic hairpin sequences studied, which include fully (10 , 11) and partly (14) matched palindromic sequences, can exist in solution as a mixture of two ordered forms identified as the monomeric hairpin and the dimeric duplex structures. In principle, the oligonucleotide psC4 could also form dimeric duplex structures with parallel orientation of the strands (Fig. 1 B), but the hyperchromicity profile and the CD spectra of the dimeric structure of psC4 are more characteristic for an antiparallel-stranded helix (6 , 7). The formation of partially base-paired antiparallel dimeric structure by psC4 (Fig. 1 C) can be excluded by the remarkable increase of the hyperchromicity in the UV melting curve by formation of the dimeric structure (Fig. 2). Furthermore a dimer with partially base-paired antiparallel structure should be very unstable and is expected to form concatamers.

Intermolecular multi-stranded helix formation

We used the FT-IR and Raman spectroscopy to probe in more detail the structure of the multi-stranded complex formed by psC4 at high salt concentration. These experiments were done at 10^{-3} M DNA concentration. Only at 1.5 mM oligomer concentration or lower and without extra addition of NaCl it was possible to observe IR spectra of psC4 characteristic for parallel-stranded structures. Upon increase of the oligomer concentration or addition of NaCl the infrared spectra of psC4 show remarkable changes, especially in the base pairing region between 1740 and 1500 cm^{-1} , indicating the formation of a new

structure. The same behaviour was also observed by Germann and co-workers (8 , 9) for a slightly different parallel-stranded hairpin structure (like mentioned above) using NMR spectroscopy. Our interpretation of the infrared spectra of psC4 leads to the conclusion that intermolecular multi-stranded structures based on a triple helix are formed by psC4 at high NaCl and/or high DNA concentrations. The triple helix is formed according to the pyrimidine motif with the third strand oriented parallel to the dA strand. Recently, Taillandier and co-workers presented IR spectra of triple helices formed by dT*dA-dT base triplets with the same strand orientation (24 , 25). They also observed an almost complete disappearance of the adenine band at about 1622 cm^{-1} , an appearance of a new band at 1633 cm^{-1} due to the thymines involved in Hoogsteen base pairing and a relatively low position of the C=O stretching vibration (mainly from C4=O4) of thymine at 1659 cm^{-1} . Furthermore the Raman spectra of psC4 compared with the apsC4 suggest triple helix formation of psC4. There is one possibility to form a triple helix according to the pyrimidine motif by two psC4 molecules (Fig. 1 D), but in this structure the second dA strand is still not involved in base pairing. A non base-paired dA is expected to show a strong band around 1622 cm^{-1} in the infrared spectra (30). In contrast, our infrared spectra of psC4 display only a very small intensity at 1622 cm^{-1} , probably due to the residual ND_2 and ring vibration of the non base-paired cytosines in the loop. Thus, we have to assume that nearly all adenine amino protons are involved in hydrogen bonds. Considering this assumption we propose the formation of a four-stranded complex by two psC4 molecules as shown in Figure 1 E. At very high DNA concentrations, the tetraplex structure may be formed preferably by multimeric chains (Fig. 1 F). The base pairing model of this asymmetric four-stranded complex is based on the pyrimidine motif of a triple helix with two bifurcated hydrogen bonds at the O4 of the thymine each directed towards one of the amino protons of both adenines (Fig. 9).

Figure 9. Proposed base pairing pattern of the four-stranded complex formed by psC4 in the stem region.

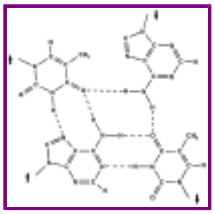

Four-stranded DNA complexes have been implicated in the pairing of homologous chromosomes during meiosis and switch recombination in immunoglobulin genes, and they may play important roles in the functioning of telomeres (31). While a large number of studies have focused on tetraplex formation of G-, and G+C-rich tracts from telomere or telomere derived sequences (32 and ref. therein), relatively little is known about four-stranded DNA complexes (tetraplexes) involving A+T tracts. Twenty-five years ago, McGavin noticed that two A[middot]T could bridge to one another forming two A(N6)-H...T (O4) hydrogen bonds across the major groove (33). Several years later, another model of a four-stranded complex was presented in which Watson-Crick base pairs were hydrogen bonded via water molecules (34). Recently, Lebrun and Lavery used molecular modelling to study conformation and energetics of four-stranded DNA complexes formed by strand exchange between duplexes (35). Their base pairing model was the same as previously suggested by McGavin (33). Some experimental evidence in favour of four-stranded complexes involving A+T tracts was obtained by Johnson and Morgan who observed reversible complexation with alternating purine-pyrimidine duplexes (36). They interpreted their data as more consistent with asymmetric base tetrads derived by adding a fourth strand to canonical TAT or CGC^+ triple helices, as we suggest for the four-stranded complex of psC4.

CONCLUSIONS

We described here the equilibrium between parallel-stranded hairpin and intermolecular dimer (multimer) of the oligonucleotide psC4 in terms of temperature, DNA and salt concentration. In contrast to the duplex formation of conventional antiparallel-stranded hairpins with short stems, the oligonucleotide psC4 can form intermolecular multi-stranded dimers (multimers) at conditions of high DNA concentration (above 1.5 mM strand) and/or higher NaCl concentrations than physiological ones. Based on our FT-IR and Raman spectroscopic data we propose the formation of an asymmetric four-stranded complex by two psC4 molecules. Interestingly, the conventional antiparallel-stranded reference hairpin apsC4 remains in the hairpin structure under all experimental conditions used. Structures similar to the described asymmetric four-stranded complex may be involved in recombination and repair processes (37).

ACKNOWLEDGEMENTS

We would like to thank C. Kraft (Max-Delbrück-Zentrum, Berlin) and J. Liquier (Laboratoire de Spectroscopie Biomoleculaire, Université Paris XIII) for the help in Raman Spectroscopy. This work was supported by the Deutsche Forschungs-gemeinschaft (DFG), Fonds der Chemischen Industrie (FCI), and the Thuringian Ministry of Science, Research and Culture.

REFERENCES

1 Pattabiraman,N. (1986) *Biopolymers*, **25**, 1603-1606.

2 Ramsing,N.B. and Jovin,T.M. (1988) *Nucleic Acids Res.*, **16**, 6659-6676.

3 Germann,M.W., Kalisch,B.W. and van de Sande,J.H. (1988) *Biochemistry*, **27**, 8302-8306.

4 Borisova,O.F., Golova, Yu.B., Gottikh,B.P., Zibrov,A.S., Il'icheva,I.A., Lysov, Yu.P., Mamayeva,O.K., Chernov,B.K., Chernyi,A.A., Shchyolkina,A.K. and Florentiev,V.L. (1991) *J. Biomol. Struct. Dyn.*, **8**, 1187-1210.

5 Rippe,K., Fritsch,V., Westhof,E. and Jovin,T.M. (1992) *EMBO J.*, **11**, 3777-3786.

6 van de Sande,J.H., Ramsing,N.B., Germann,M.W., Elhorst,W., Kalisch,B.W., v. Kitzing,E., Pon,R.T., Clegg,R.C. and Jovin,T.M. (1988) *Science*, **214**, 551-557.

7 Germann,M.W., Vogel,H.J., Pon,R.T. and van de Sande,J.H. (1990) *Biochemistry*, **29**, 9426-9432.

8 Germann,M.W., Vogel,H.J., Pon,R.T. and van de Sande,J.H. (1989) *Biochemistry*, **28**, 6220-6228.

9 Zhou,N., Germann,M.W., van de Sande,J.H., Pattabiraman,N. and Vogel,H.J. (1993) *Biochemistry*, **32**, 646-656.

10 Scheffler,I.E., Elson,E.L. and Baldwin,R.L. (1968) *J. Mol. Biol.*, **36**, 291-304.

11 Marky,L.A., Blumenfeld,K.S., Kozlowski,S. and Breslauer,K.J. (1983) *Biopolymers*, **22**, 1247-1257.

12 Haasnoot,C.A.G., Hilbers,C.W., van der Marcel,G.A., van Boom,J.H., Singh, U.C., Pattabiraman,N. and Kollmann,P.A. (1986) *J. Biol. Struct. Dyn.*, **3**, 843-857.

13 Orbons,L.P.M., van der Marcel,G.A., van Boom,J.H. and Altona,C. (1986) *Nucleic Acids Res.*, **14**, 4187-4195.

14 Roy,S., Weinstein,S., Borah,B., Nickol,J., Appella,E., Sussman,J.L., Miller,M., Shindo,H. and Cohen,J.S. (1986) *Biochemistry*, **25**, 7417-7423.

15 Xodo,L.E., Manzini,G., Quadrifoglio,F., van der Marcel,G.A. and van Boom,J.H. (1988) *Biochemistry*, **27**, 6327-6331.

16 Birch-Hirschfeld,E., Földes-Papp,Z., Gührs,K.H. and Seliger,H. (1996) *Helv. Chim. Acta.*, **79**, 137-150.

17 Ramsing,N.B., Rippe,K. and Jovin,T.M. (1989) *Biochemistry*, **28**, 9528-9535.

18 Behlke,J., Ristau,O. and Knespel,A. (1994) *Progr. Colloid Polymer Sci.*, **94**, 40-45.

19 Cohen,G. and Eisenberg,H. (1968) *Biopolymers*, **6**, 1077-1100.

20 Kauppinen,J.K., Moffatt,D.J., Mantsch,H.H. and Cameron,D.G. (1981) *Appl. Spectrosc.*, **35**, 271-276.

21 Park,Y.-W. and Breslauer,K.J. (1992) *Proc. Natl. Acad. Sci. USA*, **89**, 6653-6657.

22 Fritzsche,H., Akhebat,A., Taillandier,E., Rippe,K. and Jovin,T.M. (1993) *Nucleic Acids Res.*, **21**, 5085-5091.

23 Maher,L.J. (1992) *BioEssays*, **14**, 807-815.

24 Liquier,J., Coffinier,P., Firon,M. and Taillandier,E. (1991) *J. Biomol. Struct. Dyn.*, **3**, 437-445.

25 Dagneaux,C., Liquier,J. and Taillandier,E. (1995) *Biochemistry*, **34**, 14815-14818.

26 Otto,C., Thomas,G.A., Rippe,K., Jovin,T.M. and Peticolas,W.L. (1991) *Biochemistry*, **30**, 3062-3069.

27 Ross,P.D., Howard,F.B. and Lewis,M.S. (1991) *Biochemistry*, **30**, 6269-6275.

28 Lee,J.S., Johnson,D.A. and Morgan,A.R. (1979) *Nucleic Acids Res.*, **6**, 3073-3091.

29 Antao,V.P., Gray,D.M. and Ratliff,R.L. (1988) *Nucleic Acids Res.*, **16**, 719-738.

30 Tsuboi,M. (1969) In Brame Jr.,E.G. (ed.) *Applied Spectroscopy Rev.*, Dekker, New York, Vol. **3**, pp. 45-90.

31 Sen,D. and Gilbert,W. (1988) *Nature*, **334**, 364-366.

32 Rhodes,D. and Giraldo,R. (1995) *Curr. Opin. Struct. Biol.*, **5**, 311-322.

33 McGavin,S. (1971) *J.Mol.Biol.*, **55**, 293-298.

34 Edwards,P.A.W. (1978) *J. Theor. Biol.*, **70**, 323-334.

35 Lebrun,A. and Lavery,R. (1995) *J. Biomol. Struct. Dyn.*, **13**, 459-464.

36 Johnson,D. and Morgan,A.R. (1978) *Proc. Natl. Acad. Sci. USA*, **75**, 1637-1641.

37 Gaillard,C. and Strauss,F. (1994) *Science*, **264**, 433-436.

---

*To whom correspondence should be addressed. Tel: +49 3641 657560; Fax: +49 3641 657520; Email: hfri@hodler.molebio.uni-jena.de